Response to Paul Tackley

We thank Paul Tackley for drawing attention to the shortcomings and the possible improvements of the manuscript.

1. We stood for building up a simple analytical model based on the balance of the viscous and the buoyancy force (Jellinek and Manga, 2002) in order to compare it with our numerical results. The model applying the parameters from our simulations estimates a range for the time-variation of the concentration decrease in the lower layer. There is an uncertainty in plume velocity which depends strongly on the depth. Thus we calculated the radial velocity at the depth of 300 km (top of the initial dense layer), 400 km and 500 km above the CMB which gave $3 \cdot 10^{-11}$ m/s to 10^{-10} m/s for β=6% initial relative density contrast. This values result in 10–20 km tendril thickness and entrainment rate of the dense material of 0.85–$5.2 \cdot 10^{-18}$ 1/s which covers the slope of the decrease of the concentration of the dense layer (Fig. 1). The calculation was inserted in the Results section between lines 243–264.

2. Doubtless, the applied initial condition is a simplification of the processes occurred in the early stage of the Earth's history. Although we do not know exactly how and when the compositionally dense layer evolved in the deepest mantle, there are mechanisms which can explain the formation of the bottom dense layer (paragraph 2 in Discussion and conclusions in the revised manuscript). A plausible process from these is the crystallization of the basal magma ocean suggested by Stéphane Labrosse et al. (2007). Nevertheless, our main goal was not to imitate the mantle evolution from its formation, since the numerical model is too simple for that, but to introduce and propose a new diagnostic parameter, the effective buoyancy ratio to characterize the thermo-chemical mixing. We note that our models were not started off "cold (or at least, the same T as the layer above)", because the bottom thermal boundary layer of the preexisting mantle convection ensured an enhanced temperature. This excess temperature in thermal convection model stabilizes the value of the effective buoyancy ratio (point 3).
Besides we calculated a model with density difference of 6% to investigate the effect of the initial condition. After Paul Tackley's suggestion we ran a thermal convection model with an impermeable inner boundary at 300 km above the CMB to get a 'pre-heated' lower layer for the thermal initial condition. After reaching the quasi-steady state the dense layer was implemented to the model and the inner boundary was changed to permeable. Obviously, the initial phase (warming of the dense layer) was skipped during the simulation and the erosion phase started immediately but the slope of the concentration decrease stayed almost unchanged (*Figure I*). This resulted in that the mixing and the homogenization started earlier. We believe this initial condition for the temperature distribution is not more realistic for the Earth (as a primordial hot, dense bottom layer) only — agreeing with Paul Tackley — 'another endmember' of the initial condition applied in our model set.

3. In the last paragraph of Model description we write: 'Hence we use the lower and upper layer expression in geometrical meaning as the deepest 300 km thick part of the mantle and the overlying zone, respectively.' That is the boundary is fixed at 300 km above the CMB. Thus we do not need to calculate the radial/lateral layer deformation. To clarify this point we emphasize it in the revised manuscript mathematically as well (line 136–142):

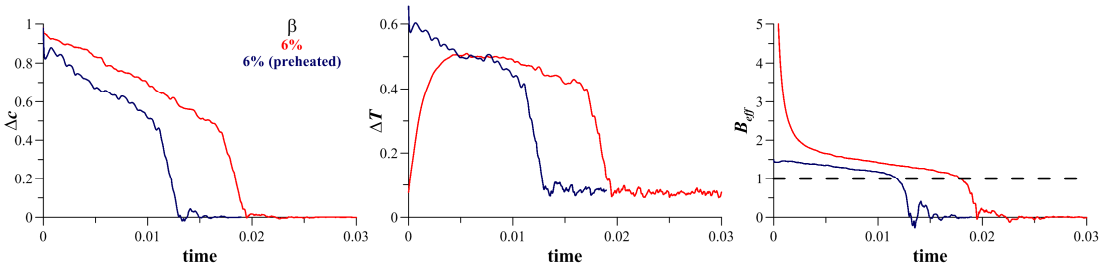

Figure I The time-variation of the concentration and the temperature difference between the layers and the effective buoyancy ratio for models with different initial temperature conditions at β=6%. Initial condition obtained from preexisting one-layer (red) and two-layer (blue) thermal convection.

$$c_0 = \frac{1}{A_0}\int_{A_0} c\,dA \quad \text{and} \quad c_1 = \frac{1}{A_1}\int_{A_1} c\,dA\,,$$

where A_0 and A_1 denote the area of the mantle above and beneath the boundary of 300 km above the CMB, respectively. Other volumetric parameters as T and v are calculated in the same manner. Therefore the concentration and temperature difference between the layers is

$$\Delta c = c_1 - c_0 \quad \text{and} \quad \Delta T = T_1 - T_0\,.$$

Peripheral parameters are determined also at fix boundaries (at CMB and surface), as well as q_D and q_{Dc} are calculated at 300 km above the CMB, too.

If the calculation of the concentration and temperature difference was based on the concentration field following the thermo-chemical mixing (e.g. the boundary was at $(c_{max}$-$c_{min})/2$ or the maximum gradient in c), B_{eff} could not track the process of homogenization. As Δc tended to zero, ΔT would converge to zero as well resulting in an unlimited solution between minus and plus infinity in B_{eff}. Due to our definition T_1-T_0>0 stands always (actually ΔT>0.07 due to the hot bottom thermal boundary layer, see in Fig. 2) that stabilizes the value of B_{eff}.

For the model of β=5% we computed B_{eff} using a different method to study its behavior when the boundary between the dense and the light material is not fixed but based on the time-dependent concentration field (*Figure II*). Namely, the boundary was defined by the contour of c=$(c_{max}$-$c_{min})/2$. Figure illustrates that the two curves are analogous to B_{eff}=1 than they diverge during the mixing and then it gives an unlimited value during the homogenization (black curve).

In addition, calculating these parameters for a fixed volume can be accomplish much more easily especially in laboratory models.

4. Two numerical tests were made based on the benchmark paper of van Keken et al. (1997) and a supplementary material was attached to the manuscript. Isoviscous model runs were carried out similarly to our systematic study. Rayleigh-Taylor instability test with analogous resolution showed that COMSOL produced good result both qualitatively and quantitatively. Due to the field method a transition in concentration field appears at large time (Fig. S1.d, t=1500), but it does not bias the quantitative values as maximum velocity, the time of maximum velocity, the growth rate and the entrainment variation.

In the thermo-chemical convection test the velocity agrees well with other results until t=0.015 then the velocities in the benchmark study tend to diverge from each other. Entrainment rate gives an acceptable agreement with other methods until t=0.04 then the mixing accelerates (Fig. S4). It is approved by the concentration field snapshots (Fig. S3)

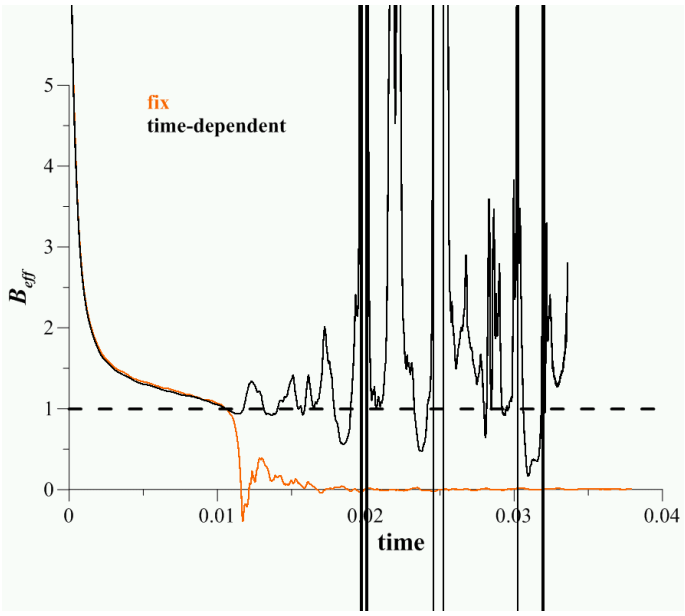

Figure II Effective buoyancy ratio calculated from fix volume of the dense/light material (orange) and from time-dependent volume based on the concentration field (black) See text for details.

where a good agreement was found to t=0.04, but at t=0.05 the entrainment of the dense material was increased.

5. The systematic models do not include internal heating since the goal of this study was to investigate the role of the effective buoyancy ratio as a parameter which characterizes the evolution of the thermo-chemical convection. In this paper we did not intend to map the effect of the different parameters, it was accomplished expansively by e.g. Deschamps and Tackley (2008, 2009) and Li et al. (2014). They investigated and established that 'The internal heating has no or very little influence on the flow pattern and the efficiency of mixing.' Analogously, investigating the entrainment rate of thermo-chemical convection in laboratory models Gonnermann et al. (2002) assumed that the entrainment rate scale with the convective velocities, so the effect of internal heating 'should not alter' their general conclusions.
Nonetheless, the internal heating likely to temperature- and depth-dependent viscosity may influence the pattern of the convection and the process of mixing. That is why we compiled and presented a more complex model including the most important ingredients (such as composition-dependent internal heating and depth-, temperature- and composition-dependent viscosity) to give an example for that.

6. The complex model was moved to Results.

Minor points:
(i) Pressure wave was modified to primary wave.
(ii) Table 2 was compiled to summarize the monitoring parameters e.g. in the left plot in Fig. 1. However, if it is needed we can repeat it in the caption of Fig. 1.
(iii) Thank you for the suggestion, the study of Gonnermann et al. (2002) was inserted into the manuscript (line 194–198).

References

Deschamps, F., and Tackley, P. J.: Searching for models of thermo-chemical convection that explain probabilistic tomography I. Principles and influence of rheological parameters, Phys. Earth Planet. Inter., 171, 357–373, 2008.
Deschamps, F., and Tackley, P. J.: Searching for models of thermo-chemical convection that explain probabilistic tomography II — Influence of physical and compositional parameters, Phys. Earth Planet. Inter., 176, 1–18, 2009.
Gonnermann, H. M., Manga, M., and Jellinek, M.: Dynamics and longevity of an initially stratified mantle, Geophys. Res. Lett., 29/10, 2002, doi:10.1029/2002GL014851.
Jellinek, A. M., and Manga, M.: The influence of a chemical boundary layer on the fixity, spacing and lifetime of mantle plumes, Nature, 418, 760–763, 2002.
Labrosse, S., Hernlund, J. W., and Coltice, N.: A crystallizing dense magma ocean at the base of the Earth's mantle, Nature, 450, 866–869, 2007.
Li, Y., Deschamps, F., Tackley, P. J.: The stability and structure of primordial reservoirs in the lower mantle: insights from models of thermochemical convection in three-dimensional spherical geometry, Geophys. J. Int., 199, 914–930, 2014.
Van Keken, P. E., King, S. D., Schmeling, H., Christensen, U. R., Neumeister, D., and Doin, M.-P.: A comparison of methods for the modeling of thermochemical convection, J. Geophys. Res., 102, 22477–22495, 1997.